

## New U–Pb Isotopic Data on the Age of Metamorphic and Igneous Rocks of the Western Margin of the Selenga–Stanovoi Orogenic Belt

A. S. Vakh<sup>a</sup>, O. V. Avchenko<sup>a</sup>, Corresponding Member of the RAS N. A. Goryachev<sup>b</sup>, V. I. Gvozdev<sup>a</sup>, V. I. Kiselev<sup>a</sup>, V. G. Khomich<sup>a</sup>, Yang Yanchen<sup>c</sup>, Ye Songqing<sup>c</sup>, and Zhang Guobin<sup>c</sup>

Received @

**Abstract**—New data on the isotopic age of zircons from metamorphic and igneous rocks are given for the Berezitovoe and Kirovskoe deposits located in the eastern margin of the Selenga–Stanovoi orogenic belt. The zircons were studied with the LA-ICP-MS method in the State Key Laboratory of Continental Dynamics, Northwestern University, Sian, Shansi province, People’s Republic of China. The results allowed us to reveal three age epochs in formation of the eastern part of the Selenga–Stanovoi orogenic belt (1.87 Ga; 380–330 Ma; 138–125 Ma), which have significant importance for understanding of the geological structure of the south-eastern framework of the North Asian craton.

DOI: 10.1134/S1028334X1306007X

This paper discusses new data on the U–Pb age of zircons from metamorphic and igneous rocks of the Kirovskoe and Berezitovoe gold fields, the geological structure of which is reviewed in detail in [3, 4], and which are located at the eastern margin of the Selenga–Stanovoi orogenic belt. The zircons were studied with LA-ICP-MS in the State Key Laboratory of Continental Dynamics, Northwestern University, Sian (Shansi province, PRC) on an Agilent 7500a mass spectrometer with inductively coupled plasma connected with a ComPex102-type ArF laser ablation system. The main results of the U–Pb dating of zircons from various rocks are shown in Table 1.

Metamorphic rocks of the Mogocha Group represented by amphibole and biotite–amphibole crystal schists and gneisses are the most ancient rocks of the eastern part of the Selenga–Stanovoi belt. They compose the Urusha–Mogocha inlier of the crystal granulitic basement. Their age is considered to be  $3600 \pm 60$  Ma [5]. Xenomorphic round semitransparent zircons from amphibole gneisses of the southern part of the Berezitovoe ore field have a complicated internal structure caused by homogeneous light and dark domains of various shapes (Fig. 2). Their isotopic age calculated by 11 points is  $1867 \pm 8.1$  Ma (Fig. 3).

In addition, five points with an older age from 2200 to 2400 Ma were revealed. The upper age boundary of 1.87 Ga for gneisses of the Mogocha Group is quite consistent with data of other researchers [5, 6] about the time of high-temperature and high-pressure metamorphism in the rocks of the southeastern frame of the North Asian craton.

The plutons of ancient granitic rocks referred to the Late Stanovoi complex on the modern geological maps are in the geological structure of both gold fields. The age of ancient granitic rocks of the Late Stanovoi complex is considered to be Early Proterozoic [2]; however, based on U–Pb isotopic studies, Late Paleozoic (340–330 Ma [7]) or Late Mesozoic (142–138 Ma [8, 9]) ages were determined for these rocks. The analyzed homogenous prismatic zircons from gneiss-like granitic rocks of this complex developed in the area of the Kirovskoe and Berezitovoe ore fields contain clearly expressed homogeneous core and rims with growth zoning (Fig. 2). Their isotopic age is similar for both deposits:  $379.0 \pm 1.1$  and  $382.8 \pm 12$  Ma for the Berezitovoe and Kirovskoe deposits, respectively (Fig. 3).

The Khaiktin pluton, mostly composed of biotite–hornblende granodiorites and granites with typical coarse porphyritic tabular grains of pink feldspar, is the greatest Mesozoic magmatic product within the Berezitovoe ore field. On the modern geological maps, the rocks of the Khaiktin pluton are referred to the Late Jurassic Amudzhikan complex of subalkaline granites [2]. At the same time, some researchers consider that igneous rocks of the pluton represent the independent Early Mesozoic Khaiktin complex of granites of the Upper Amur region, whose Rb–Sr and K–Ar age is  $132 \pm 3$  Ma [10].

<sup>a</sup> Far East Geological Institute, Far East Branch, Russian Academy of Sciences, pr. 100-letiya 159, Vladivostok, 690022 Russia

<sup>b</sup> Northeastern Complex Scientific–Research Institute, Far East Branch, Russian Academy of Sciences, ul. Portovaya 16, Magadan, 685000 Russia

<sup>c</sup> College of Earth Sciences, Jilin University, Jianshe str, 2199, Changchun, 130061 People’s Republic of China

Results of U–Pb isotopic studies of zircons from metamorphic and igneous rocks of the Selenga–Stanovoi foldbelt of the Upper Amur region: LA-ICP-MS data

Sample number	Analysis points	Measured isotopic ratios			Age, Ma	
		$\frac{^{207}\text{Pb}}{^{206}\text{Pb}}$	$\frac{^{207}\text{Pb}}{^{235}\text{U}}$	$\frac{^{206}\text{Pb}}{^{238}\text{U}}$	$\frac{^{207}\text{Pb}}{^{235}\text{U}}$	$\frac{^{206}\text{Pb}}{^{238}\text{U}}$
1721	1	0.1055 ± 0.002	4.8978 ± 0.41	0.3356 ± 0.004	1802 ± 70	1866 ± 18
	2	0.1052 ± 0.001	4.8878 ± 0.32	0.3356 ± 0.002	1800 ± 54	1865 ± 9
	3	0.1120 ± 0.002	5.2231 ± 0.26	0.3365 ± 0.003	1856 ± 43	1870 ± 16
	4	0.1098 ± 0.001	5.1016 ± 0.16	0.3362 ± 0.002	1836 ± 27	1868 ± 8
	5	0.1518 ± 0.001	9.4652 ± 0.18	0.4510 ± 0.003	2384 ± 18	2400 ± 15
	6	0.1401 ± 0.001	8.7336 ± 0.10	0.4513 ± 0.002	2311 ± 10	2401 ± 10
	7	0.1243 ± 0.001	7.3233 ± 0.09	0.4271 ± 0.003	2152 ± 11	2293 ± 12
	8	0.1517 ± 0.001	9.4682 ± 0.16	0.4510 ± 0.004	2384 ± 15	2400 ± 19
	9	0.1108 ± 0.002	5.1422 ± 0.11	0.3361 ± 0.003	1843 ± 19	1868 ± 16
	10	0.0518 ± 0.001	0.4347 ± 0.01	0.0607 ± 0.001	366 ± 8	380 ± 2
	11	0.0507 ± 0.001	0.4271 ± 0.01	0.0608 ± 0.001	361 ± 7	380 ± 3
	12	0.0987 ± 0.002	4.5771 ± 0.11	0.3361 ± 0.003	1745 ± 19	1868 ± 17
	13	0.1121 ± 0.001	5.2062 ± 0.10	0.3362 ± 0.003	1854 ± 16	1869 ± 14
	14	0.1102 ± 0.001	5.1011 ± 0.09	0.3357 ± 0.003	1836 ± 14	1866 ± 16
	15	0.1148 ± 0.002	5.4548 ± 0.11	0.3460 ± 0.005	1894 ± 17	1915 ± 24
	16	0.1106 ± 0.001	5.1221 ± 0.10	0.3362 ± 0.004	1840 ± 17	1868 ± 21
	17	0.1453 ± 0.001	9.0425 ± 0.19	0.4510 ± 0.004	2342 ± 19	2400 ± 16
	18	0.1132 ± 0.004	5.0970 ± 0.15	0.3364 ± 0.005	1836 ± 26	1869 ± 24
	19	0.1055 ± 0.002	4.8795 ± 0.19	0.3360 ± 0.004	1799 ± 32	1867 ± 18
	20	0.1064 ± 0.002	5.0793 ± 0.23	0.3460 ± 0.004	1833 ± 39	1915 ± 18
1701	1	0.0505 ± 0.000	0.4240 ± 0.008	0.0606 ± 0.000	359 ± 6	379 ± 1
	2	0.0557 ± 0.002	0.4686 ± 0.019	0.0606 ± 0.001	390 ± 13	379 ± 4
	3	0.0489 ± 0.001	0.4113 ± 0.013	0.0606 ± 0.000	350 ± 10	379 ± 2
	4	0.0483 ± 0.001	0.4058 ± 0.016	0.0606 ± 0.000	346 ± 11	379 ± 3
	5	0.0474 ± 0.001	0.3992 ± 0.018	0.0606 ± 0.001	341 ± 13	380 ± 4
	6	0.0547 ± 0.001	0.5306 ± 0.033	0.0678 ± 0.002	432 ± 22	423 ± 11
	7	0.0469 ± 0.001	0.3944 ± 0.020	0.0606 ± 0.000	338 ± 14	379 ± 2
	8	0.0482 ± 0.000	0.4045 ± 0.024	0.0606 ± 0.001	345 ± 17	379 ± 4
	9	0.0561 ± 0.001	0.5838 ± 0.060	0.0687 ± 0.003	467 ± 39	428 ± 18
	10	0.0488 ± 0.001	0.4092 ± 0.035	0.0605 ± 0.001	348 ± 25	379 ± 3
	11	0.0490 ± 0.001	0.4147 ± 0.036	0.0606 ± 0.001	352 ± 26	379 ± 5
	12	0.0486 ± 0.001	0.4075 ± 0.028	0.0606 ± 0.000	347 ± 20	379 ± 2
	13	0.0486 ± 0.001	0.4079 ± 0.022	0.0606 ± 0.000	347 ± 16	379 ± 2
	14	0.0585 ± 0.007	0.6616 ± 0.071	0.0821 ± 0.003	516 ± 43	509 ± 21
	15	0.0497 ± 0.001	0.4752 ± 0.019	0.0688 ± 0.001	395 ± 13	429 ± 7
	16	0.0498 ± 0.001	0.4192 ± 0.017	0.0607 ± 0.001	355 ± 12	380 ± 7
	17	0.0484 ± 0.000	0.4078 ± 0.018	0.0606 ± 0.000	347 ± 13	379 ± 2
	18	0.0470 ± 0.001	0.3943 ± 0.024	0.0606 ± 0.001	338 ± 17	379 ± 4
	19	0.0493 ± 0.001	0.4215 ± 0.034	0.0607 ± 0.001	357 ± 25	380 ± 6
	20	0.0450 ± 0.001	0.3789 ± 0.037	0.0606 ± 0.001	326 ± 27	379 ± 3

Table. (Contd.)

Sample number	Analysis points	Measured isotopic ratios			Age, Ma	
		$\frac{^{207}\text{Pb}}{^{206}\text{Pb}}$	$\frac{^{207}\text{Pb}}{^{235}\text{U}}$	$\frac{^{206}\text{Pb}}{^{238}\text{U}}$	$\frac{^{207}\text{Pb}}{^{235}\text{U}}$	$\frac{^{206}\text{Pb}}{^{238}\text{U}}$
K-2	1	0.0499 ± 0.001	0.4220 ± 0.009	0.0613 ± 0.000	357 ± 6	383 ± 3
	2	0.0668 ± 0.002	0.7015 ± 0.025	0.0750 ± 0.001	540 ± 15	466 ± 6
	3	0.0575 ± 0.001	0.4853 ± 0.009	0.0613 ± 0.000	402 ± 6	383 ± 2
	4	0.0512 ± 0.001	0.4323 ± 0.008	0.0613 ± 0.000	365 ± 5	383 ± 2
	5	0.0556 ± 0.002	0.4681 ± 0.014	0.0611 ± 0.000	390 ± 10	382 ± 3
	6	0.0620 ± 0.001	0.5256 ± 0.010	0.0613 ± 0.000	429 ± 7	384 ± 3
	7	0.0532 ± 0.001	0.4497 ± 0.009	0.0613 ± 0.001	377 ± 6	383 ± 3
	8	0.0570 ± 0.001	0.4630 ± 0.011	0.0588 ± 0.000	386 ± 8	368 ± 2
	9	0.0502 ± 0.001	0.4264 ± 0.009	0.0613 ± 0.000	361 ± 6	383 ± 2
	10	0.0497 ± 0.001	0.4216 ± 0.010	0.0612 ± 0.000	357 ± 7	383 ± 2
	11	0.0499 ± 0.001	0.4223 ± 0.012	0.0612 ± 0.001	358 ± 8	383 ± 5
	12	0.0520 ± 0.001	0.4409 ± 0.011	0.0613 ± 0.001	371 ± 8	383 ± 4
	13	0.0502 ± 0.001	0.5195 ± 0.012	0.0749 ± 0.000	425 ± 8	465 ± 3
	14	0.0501 ± 0.001	0.4208 ± 0.011	0.0610 ± 0.000	357 ± 8	381 ± 2
	15	0.0550 ± 0.001	0.4650 ± 0.014	0.0612 ± 0.000	388 ± 9	383 ± 2
	16	0.0493 ± 0.001	0.4184 ± 0.014	0.0614 ± 0.001	355 ± 10	384 ± 5
	17	0.0518 ± 0.001	0.4391 ± 0.014	0.0613 ± 0.001	370 ± 10	383 ± 3
	18	0.0507 ± 0.001	0.4290 ± 0.014	0.0612 ± 0.001	362 ± 10	383 ± 4
	19	0.0488 ± 0.001	0.4150 ± 0.013	0.0612 ± 0.000	352 ± 10	383 ± 2
	20	0.0565 ± 0.001	0.4788 ± 0.019	0.0613 ± 0.000	397 ± 13	383 ± 3
15	1	0.0445 ± 0.001	0.1320 ± 0.004	0.0215 ± 0.000	126 ± 3	137 ± 1
	2	0.0455 ± 0.001	0.1372 ± 0.004	0.0218 ± 0.000	131 ± 3	139 ± 1
	3	0.0477 ± 0.001	0.1411 ± 0.003	0.0214 ± 0.000	134 ± 3	137 ± 1
	4	0.0484 ± 0.001	0.1452 ± 0.003	0.0218 ± 0.000	138 ± 3	139 ± 1
	5	0.0609 ± 0.001	0.1799 ± 0.004	0.0215 ± 0.000	168 ± 3	137.1 ± 1
	6	0.0466 ± 0.001	0.1369 ± 0.003	0.0214 ± 0.000	130 ± 3	136 ± 1
	7	0.0477 ± 0.001	0.1408 ± 0.004	0.0214 ± 0.000	134 ± 4	137 ± 1
	8	0.0457 ± 0.001	0.1305 ± 0.005	0.0208 ± 0.000	125 ± 4	132.4 ± 0.9
	9	0.1051 ± 0.000	3.9837 ± 0.180	0.2735 ± 0.003	1631 ± 37	1558 ± 16
	10	0.0499 ± 0.001	0.1613 ± 0.010	0.0235 ± 0.000	152 ± 8	150 ± 1
	11	0.0461 ± 0.026	1.5692 ± 0.893	0.2472 ± 0.008	958 ± 353	1424 ± 42
	12	0.0584 ± 0.001	0.1920 ± 0.010	0.0237 ± 0.000	178 ± 8	151 ± 1
	13	0.0466 ± 0.001	0.1343 ± 0.005	0.0209 ± 0.000	128 ± 5	133.2 ± 0.9
	14	0.0495 ± 0.001	0.1477 ± 0.005	0.0215 ± 0.000	140 ± 4	137 ± 1
	15	0.0514 ± 0.001	0.1528 ± 0.004	0.0214 ± 0.000	144 ± 4	136 ± 1
	16	0.0477 ± 0.001	0.1421 ± 0.003	0.0217 ± 0.000	135 ± 3	138 ± 1
	17	0.0485 ± 0.001	0.1457 ± 0.003	0.0217 ± 0.000	138 ± 3	139 ± 1
	18	0.0482 ± 0.001	0.1443 ± 0.003	0.0216 ± 0.000	137 ± 3	138 ± 1
	19	0.0529 ± 0.001	0.1595 ± 0.003	0.0217 ± 0.000	150 ± 3	139 ± 1
	20	0.0511 ± 0.001	0.3495 ± 0.011	0.0495 ± 0.001	304 ± 8	312 ± 9

Table. (Contd.)

Sample number	Analysis points	Measured isotopic ratios			Age, Ma	
		$\frac{^{207}\text{Pb}}{^{206}\text{Pb}}$	$\frac{^{207}\text{Pb}}{^{235}\text{U}}$	$\frac{^{206}\text{Pb}}{^{238}\text{U}}$	$\frac{^{207}\text{Pb}}{^{235}\text{U}}$	$\frac{^{206}\text{Pb}}{^{238}\text{U}}$
PR-1	1	0.0468 ± 0.002	0.1557 ± 0.008	0.0246 ± 0.000	147 ± 7	157 ± 2
	2	0.0506 ± 0.001	0.1732 ± 0.005	0.0246 ± 0.000	162 ± 5	156 ± 2
	3	0.0454 ± 0.001	0.1319 ± 0.003	0.0209 ± 0.000	126 ± 3	134 ± 1
	4	0.0577 ± 0.010	0.1394 ± 0.004	0.0216 ± 0.000	132 ± 3	138 ± 2
	5	0.0482 ± 0.001	0.1412 ± 0.004	0.0214 ± 0.000	134 ± 3	136 ± 2
	6	0.0487 ± 0.001	0.1408 ± 0.003	0.0210 ± 0.000	134 ± 3	133.7 ± 0.8
	7	0.0496 ± 0.001	0.4184 ± 0.008	0.0611 ± 0.000	355 ± 6	382 ± 2
	8	0.0457 ± 0.001	0.1548 ± 0.005	0.0246 ± 0.000	146 ± 4	157 ± 2
	9	0.0566 ± 0.001	0.1660 ± 0.006	0.0210 ± 0.000	156 ± 5	134 ± 1
	10	0.0493 ± 0.001	0.1429 ± 0.005	0.0209 ± 0.000	136 ± 4	133.4 ± 0.7
	11	0.0591 ± 0.001	0.4993 ± 0.017	0.0614 ± 0.001	411 ± 12	384 ± 4
	12	0.0417 ± 0.000	0.1205 ± 0.003	0.0209 ± 0.000	116 ± 3	133.2 ± 0.7
	13	0.0426 ± 0.001	0.1448 ± 0.004	0.0245 ± 0.000	137 ± 4	156 ± 2
	14	0.0465 ± 0.001	0.1362 ± 0.005	0.0209 ± 0.000	130 ± 5	133 ± 2
	15	0.0399 ± 0.001	0.1151 ± 0.003	0.0209 ± 0.000	111 ± 3	133.4 ± 0.8
	16	0.0400 ± 0.001	0.1154 ± 0.003	0.0209 ± 0.000	111 ± 3	133.2 ± 0.7
	17	0.0451 ± 0.001	0.1305 ± 0.004	0.0209 ± 0.000	125 ± 3	133 ± 1
	18	0.0442 ± 0.001	0.1272 ± 0.003	0.0209 ± 0.000	122 ± 3	133 ± 0.8
	19	0.0441 ± 0.001	0.1277 ± 0.004	0.0209 ± 0.000	122 ± 3	133 ± 1
	20	0.0524 ± 0.011	0.1846 ± 0.037	0.0256 ± 0.000	172 ± 32	163 ± 2
K-1	1	0.0512 ± 0.002	0.1382 ± 0.005	0.0196 ± 0.000	131 ± 5	125 ± 1
	2	0.0466 ± 0.002	0.1253 ± 0.006	0.0196 ± 0.000	120 ± 5	125 ± 1
	3	0.0505 ± 0.004	0.1459 ± 0.011	0.0209 ± 0.000	138 ± 10	134 ± 3
	4	0.0503 ± 0.002	0.1364 ± 0.005	0.0196 ± 0.000	130 ± 5	125 ± 1
	5	0.0579 ± 0.002	0.1758 ± 0.008	0.0220 ± 0.001	164 ± 7	141 ± 4
	6	0.0477 ± 0.003	0.1277 ± 0.007	0.0194 ± 0.000	122 ± 7	124 ± 2
	7	0.0501 ± 0.004	0.1345 ± 0.009	0.0195 ± 0.000	128 ± 8	124 ± 2
	8	0.1189 ± 0.023	2.5566 ± 0.432	0.1559 ± 0.013	1288 ± 123	934 ± 75
	9	0.0505 ± 0.004	0.1630 ± 0.012	0.0234 ± 0.000	153 ± 10	149 ± 2
	10	0.0536 ± 0.002	0.1429 ± 0.006	0.0196 ± 0.000	136 ± 5	125 ± 2
	11	0.0585 ± 0.006	0.1608 ± 0.016	0.0200 ± 0.000	151 ± 14	127 ± 2
	12	0.0479 ± 0.002	0.1300 ± 0.007	0.0196 ± 0.000	124 ± 6	125 ± 1
	13	0.0461 ± 0.067	0.1562 ± 0.227	0.0246 ± 0.003	147 ± 199	157 ± 17
	14	0.0504 ± 0.003	0.1380 ± 0.008	0.0199 ± 0.000	131 ± 7	127 ± 2
	15	0.0498 ± 0.002	0.1336 ± 0.005	0.0196 ± 0.000	127 ± 5	125 ± 1
	16	0.0502 ± 0.005	0.1576 ± 0.014	0.0228 ± 0.001	149 ± 12	145 ± 3
	17	0.0531 ± 0.002	0.1434 ± 0.005	0.0198 ± 0.000	136 ± 4	126 ± 2
	18	0.0548 ± 0.005	0.1509 ± 0.014	0.0200 ± 0.000	143 ± 13	128 ± 2
	19	0.0672 ± 0.018	0.1836 ± 0.041	0.0196 ± 0.000	171 ± 36	125 ± 3
	20	0.0538 ± 0.007	0.1461 ± 0.020	0.0197 ± 0.000	138 ± 17	126 ± 1

Note: Amphibole gneiss (1721); gneiss-like biotite–hornblende granodiorite, Berezitovoe ore field (1701); gneiss-like biotite–hornblende granite, Kirovskoe ore field (K-2); coarse porphyritic biotite–hornblende granite, Khaiktin pluton (15); porphyry granosyenite, Peral'noe occurrence (PR-1); granodiorite of the Dzhailinda pluton (K-1). Analyses were performed in the State Laboratory of Continental Dynamics, Northwest University, Sian, Shansi province, PRC.

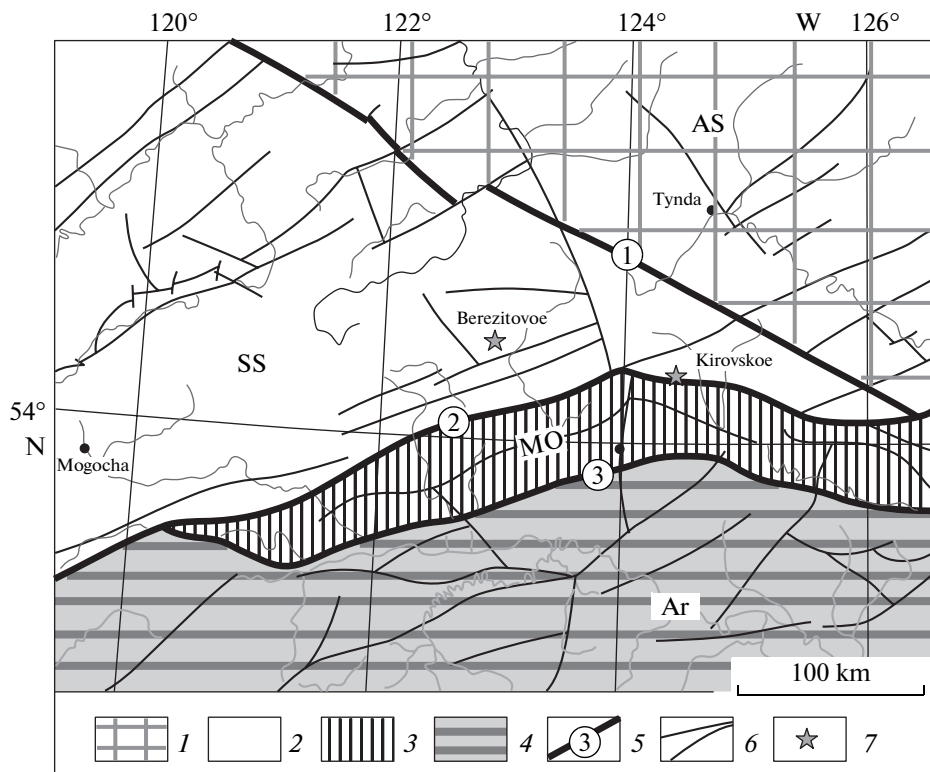


**Fig. 1.** Location of the Berezitovoe and Kirovskoe gold deposits of the Upper Amur region in structures of the southeastern frame of the North Asian craton, composed after [1, 2]. (1) Aldan–Stanovoi shield (AS); (2–4) orogenic belts: (2) Selenga–Stanovoi (SS), (3) Mongol–Okhotsk (MO), (4) Argun (Ar); (5) major regional faults: Dzheltulak (1), North Tukuringra (2), South Tukuringra (3); (6) faults; (7) gold deposits.

The accessory zircons from coarse porphyritic granites of the Khaiktin pluton are semitransparent long prismatic well-faceted dipyrnid crystals with a clearly expressed thin oscillatory zoning (Fig. 2). Their concordant age calculated by 13 points is  $137.62 \pm 0.67$  Ma.

The development of subvolcanic sills and dikes of porphyry granites and porphyry granosyenites is related to the final stage of formation of granitic rocks of the Amudzhikan complex. Two varieties of zircons distinct in morphology and internal structure were identified in the sample of ore-bearing porphyry granosyenite from the Pereval'noe Au–Mo porphyry occurrence (Fig. 2). The age of the majority of zircons from porphyry granosyenites is  $135 \pm 3.3$  Ma (Fig. 3). The concordant age of another zircon variety is  $157 \pm 3.7$  Ma, which indicates its xenogenic origin.

The Dzhhalinda intrusion, hosting the main ore bodies of the Kirovskoe deposit in the southern part, is mostly composed of granodiorites and porphyry granites. The age of intrusion and associated gold mineralization was previously considered as Early Cretaceous, i.e., 131–126 Ma (Rb–Sr method [11]) or 128–125 Ma ( $^{40}\text{Ar}/^{39}\text{Ar}$  method [12]). Zircons extracted from the sample of granodiorites of the southern part of the Dzhhalinda pluton include colorless transparent

elongated dipyrnid crystals. They are characterized by a homogeneous core and lighter rim (Fig. 2). Their concordant age is  $125.44 \pm 0.69$  Ma, which generally corresponds to the previously published data.

The analysis of isotopic results of zircons allows us to distinguish three main epochs in the evolution of the eastern part of the Selenga–Stanovoi belt. The oldest event (1.87 Ga) dated by zircons from metamorphic rocks reflects the regional tectono-magmatic process that resulted in significant transformation of the basement rocks of the Selenga–Stanovoi belt. It coincides with the epoch of the regional metamorphism of amphibolite facies of the rocks of the Dzhugdzhur–Stanovoi belt [6]. The following epoch of 380–330 Ma characterizes the formation of the Late Paleozoic igneous rocks during granitization of metamorphic rocks in the eastern part of the Selenga–Stanovoi belt. It should be noted that Paleozoic magmatic manifestations should be considered as one of the typical peculiarities of the geological structure of the eastern part of the Selenga–Stanovoi belt, because no similar rocks were identified in the adjacent territory of the Aldan–Stanovoi shield (eastward from the Dzheltulak fault). The third event (138–125 Ma) characterizes the global epoch of the Early Cretaceous granitic formation within the eastern part of the

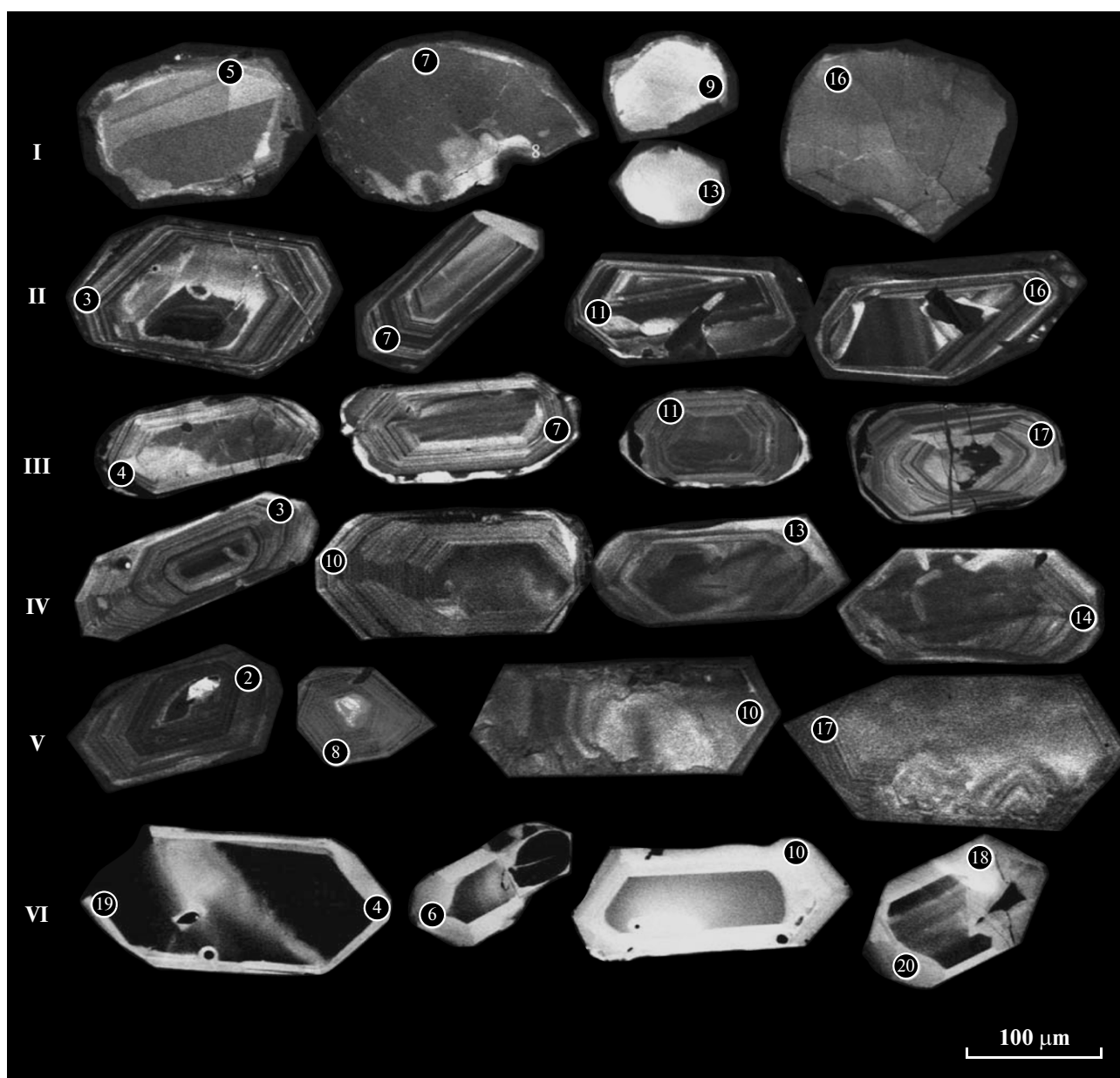


**Fig. 2.** Cathodoluminescent images of individual analyzed zircon aggregates from metamorphic and igneous rocks of the eastern part of the Selenga–Stanovoi area. (I) Amphibole gneiss of the Mogocha Group (sample 1721), (II) gneiss-like biotite–hornblende granodiorite of the Late Stanovoi complex, Berezitovoe ore field (sample 1701), (III) gneiss-like biotite–hornblende granodiorite of the Late Stanovoi complex, Kirovskoe ore field (sample K-2), (IV) coarse porphyritic biotite–hornblende granite of the Amudzhikan complex, Khaiktin pluton (sample 15), (V) porphyry granosyenite of the Amudzhikan complex, Perval'noe Au–Mo porphyry occurrence (sample PR-1), (VI) granodiorite of the Dzhailinda pluton, Kirovskoe ore field (sample K-1). Numbers of analyses correspond to the numbers in the table.

Selenga–Stanovoi belt with clearly expressed gold occurrences, the formation of which occurred at the transform continental margin [13]. It should be emphasized that the U–Pb age of zircons from the Mesozoic gold-bearing igneous complexes decreases eastward within the given structure, from the Middle to Late Jurassic in the central part (gold objects of the

Western Transbaikalia) to the Early Cretaceous in the east (Upper Amur region).

Thus, the results of isotopic study of zircons from rocks widespread on gold-bearing fields of the Upper Amur region allowed us to reveal the major age epochs in the evolution of the eastern part of the Selenga–Stanovoi orogenic belt, which have principal signifi-

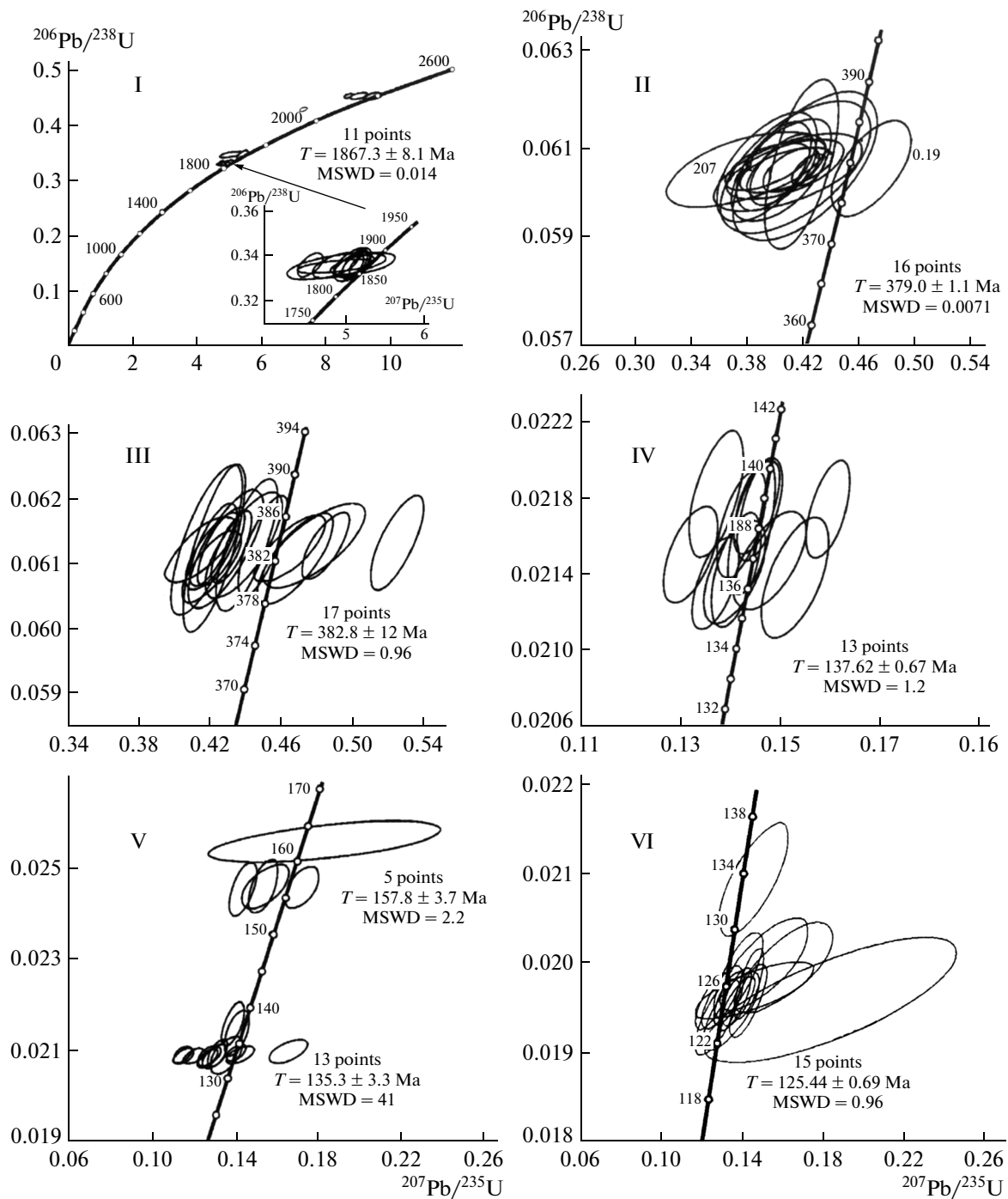


**Fig. 3.** U–Pb isotopic plots with concordia for zircons from metamorphic and igneous rocks of the eastern margin of the Selenga–Stanovoi orogenic belt. The inset plot shows the fragment of the concordia in the area of the age range of 1750–1950 Ma; I–VI, see Fig. 2.

cance for the solution of geological, tectonic, and metallogenic problems of the southeastern framework of the North Asian craton.

#### ACKNOWLEDGMENTS

This study was supported by the Far East Branch, Russian Academy of Sciences (project nos. 12-III-A-

08-145, 12-III-A-08-146, 12-III-SO-08-030, 12-I-P27-02, and 12-3-A08-159).

#### REFERENCES

1. *Geological map of the Amur region and adjacent territories on a scale of 1 : 2 500 000. Explanatory report*, Ed. by

- L.I. Krasnyi and Pen Yun'byao (St-Petersburg, Blagoveshchensk, Harbin, 1999) [in Russian].
2. Z. P. Kozak and K. D. Vakhtomin, *State geological map of Russian Federation on a scale of 1 : 200 000. Second edition. Stanovaya series. N-51-XIV (Takhtamygda)* (VSEGEI, St. Petersburg, 2000) [in Russian].
3. V. G. Moiseenko and L. V. Eirish, *Gold deposits of the East of Asia* (Dal'nauka, Vladivostok, 1996) [in Russian].
4. A. S. Vakh, V. A. Stepanov, and O. V. Avchenko, *Rudy Met.*, No. 6, 44–55 (2008).
5. S. N. Gavrikova, L. A. Nikolaeva, A. V. Galanin, et al., *Early Precambrian of the southern part of the Stanovoi fold area* (Nedra, Moscow, 1991) [in Russian].
6. A. P. Nutman, I. V. Chernyshev, and H. Baadsgaard, *Precambrian Res.* **54**, 195–210 (1992).
7. A. S. Vakh, O. V. Avchenko, S. A. Sergeev, et al., *Dokl. Akad. Nauk* **438** (2), 819–824 (2011).
8. A. M. Larin, A. B. Kotov, E. B. Sal'nikova, et al., *Petrologiya* **9** (4), 362–375 (2001).
9. A. M. Larin, E. B. Sal'nikova, A. B. Kotov, et al., *Dokl. Akad. Nauk* **409** (1), 727–731 (2006).
10. V. E. Strikha, N. N. Petruk, K. D. Vakhtomin, et al., *Tikhookean. Geol.*, No. 5, 25–37 (2000).
11. V. G. Moiseenko, V. A. Stepanov, and Yu. P. Shergina, *Dokl. Akad. Nauk* **369** (9), 1217–1219 (1999).
12. A. A. Sorokin, V. A. Ponomarchuk, A. V. Travin, et al., in *Proceeding of the Second All-Russian Scientific Conference on Problems of geology and complex exploration of the natural resources of the Eastern Asia* (IGP DVO RAN, Blagoveshchensk, 2012), p. 57–58 [in Russian].
13. *Geodynamics, magmatism, and metallogeny of the Russian East* Ed. by A.I. Khanchuk (Dal'nauka, Vladivostok, 2006) [in Russian].

**SPELL OK**